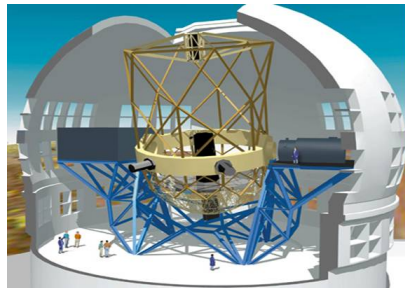
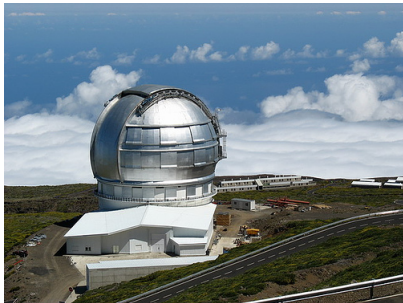


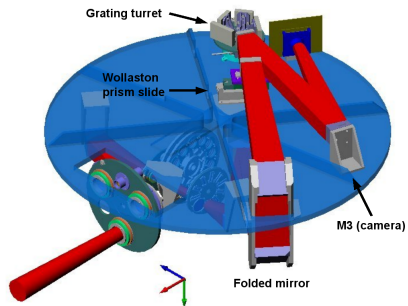
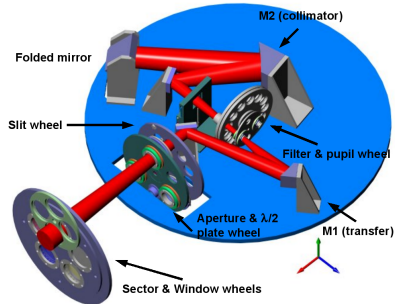
- CanariCam is a mid-infrared imager with spectroscopic, coronagraphic, and polarimetric capabilities.
- It is optimized for excellent image quality across the 8-26 μm window. The optical design is such that CanariCam is diffraction limited at 8 μm (Nyquist sampling the 8 m PSF).

Gran telescopio de canarias (GTC)

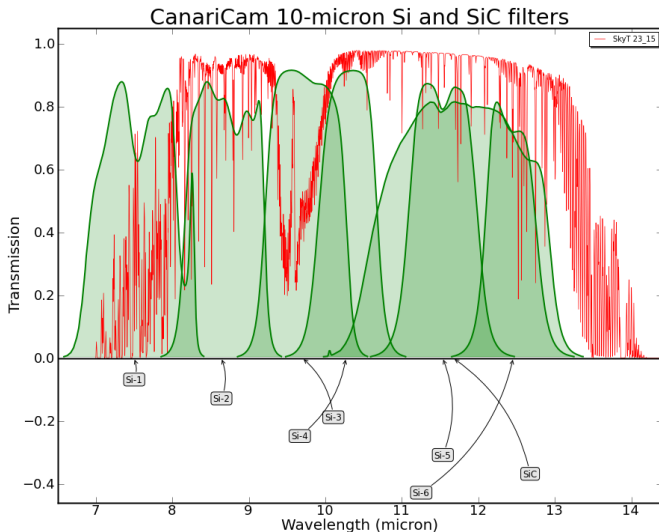


- There are three powered mirrors and five folding flats (four fixed and one movable on the grating turret). All the mirrors are gold coated, which provides a combined reflectivity of 92%.
- CanariCam is equipped with a suite of narrow-band and broad-band 10 and 20 μm filters, located within two filter wheels immediately after the Lyot-stop wheel at the first pupil image.

Optical Layout



Sky transmission and filters

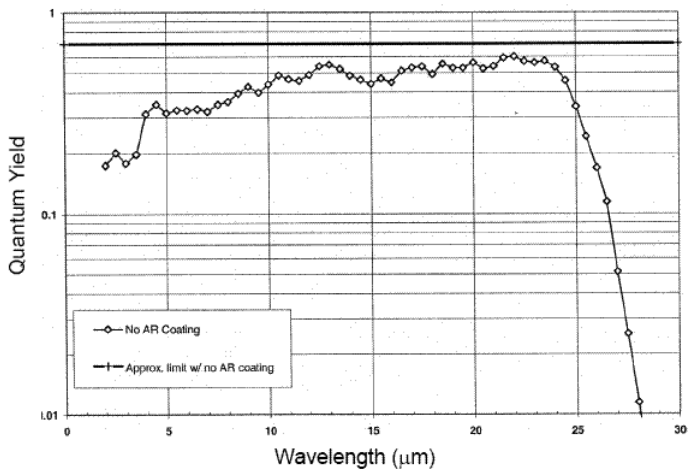


Detector characteristics

| | |
|----------------------------|--|
| Detector | Raytheon CRC-774 320x24 Si:As |
| Field of view | 25.6"x19.2" |
| Physical pixel size | 50x50 μm (0.0798") |
| Dark current | < 100 electrons/sec, T=6K |
| Quantum yield | > 40% at peak number of output channels: 16 |

Quantum efficiency of detector

Raytheon CRC-774 320×240 Sensor Chip Assembly



Spectroscopy

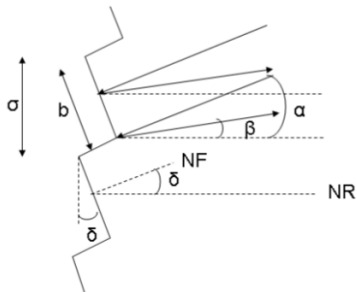
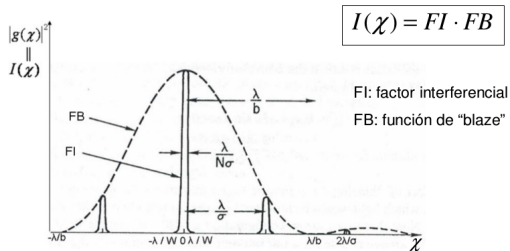
R (spectral resolution) = $\frac{\lambda}{\delta\lambda}$ is an adimensional measure of $\delta\lambda$ (spectral purity or spectral resolution element): the smallest measurable wavelength difference at a given wavelength

$R \propto \frac{\lambda A}{\min(w, l_0)}$ and $A = \frac{d\beta}{d\lambda}$ is a decreasing function of λ

| Slit Width [arcsec] | Slit Width [pixels] | GTC Diffraction Limited λ_{central} [micron] |
|------------------------|------------------------|--|
| 0.17 | 2.08 | 7.0 |
| 0.20 | 2.45 | 8.3 |
| 0.23 | 2.85 | 9.5 |
| 0.26 | 3.25 | 10.7 |
| 0.36 | 4.31 | 14.9 |
| 0.41 | 5.01 | 16.9 |
| 0.45 | 5.70 | 18.6 |
| 0.52 | 6.50 | 21.5 |
| 1.04 | 13.0 | seeing limited |

Typically for each grating there will be 2 slits available corresponding to the resolution and two times the resolution at the maximum wavelength (1 and 2 λ/D)

Spectroscopy



- $W = \sigma N$, $b = \sigma \cos \delta$, $\chi = \sin \alpha + \sin \beta$
- FI max when $\frac{m\lambda}{\sigma} = \sin \alpha + \sin \beta$
- FB max when $\alpha + \beta = 2\delta$
- α, δ fixed \implies max intensity when
 $\beta = 2\delta - \alpha \implies \lambda_{max} = \frac{\sigma}{m}(\sin \alpha + \sin(2\delta - \alpha))$ which for $m = 1$ is
called λ_{blaze}

10 μ window (7.5 - 13.5 μm also called N band) low and high resolution grating

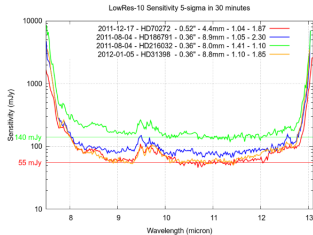
| Characteristics | LR | HR |
|---|------|--|
| Central $\lambda_c(\mu m)$ | 10.5 | 10.5 |
| Blaze $\lambda(\mu m)$ | 9.87 | 10.08 |
| Blaze Angle ($^\circ$) | 2.6 | 16.4 |
| Lines/mm(N) | 9.1 | 56.0 |
| $\delta\lambda_{Det}(\mu m)$ | 6 | 0.98 (0.65 for $\lambda_c = 10.5\mu m$) |
| Angle of incidence ($^\circ$) | 14.8 | 29.5 |
| Angle diffraction ($^\circ$) at λ_c | 9.2 | 5.5 |
| R | 175 | 1300 |
| Smallest Resolvable $\delta\lambda(\mu m)$ | 0.06 | 0.008 |

20 μ window (16.0 - 25.0 μm) low and high resolution grating

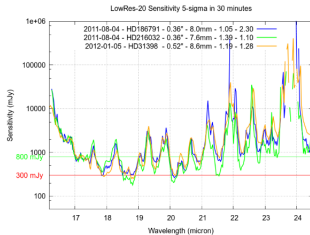
| Characteristics | LR | HR |
|---|-------|--|
| Central $\lambda_c(\mu m)$ | 20.5 | 20.5 |
| Blaze $\lambda(\mu m)$ | 19.96 | 20.18 |
| Blaze Angle ($^\circ$) | 4.0 | 20.8 |
| Lines/mm(N) | 6.1 | 35.2 |
| $\delta\lambda_{Det}(\mu m)$ | 9 | 1.54 (0.45 μm for $\lambda_c = 20.5\mu m$) |
| Angle of incidence ($^\circ$) | 15.7 | 33.7 |
| Angle diffraction ($^\circ$) at λ_c | 8.3 | 9.7 |
| R | 120 | 890 |
| Smallest Resolvable $\delta\lambda(\mu m)$ | 0.17 | 0.025 |

Spectrum dispersed along the long axis of the array (320 pixels)
Each resolution element is sampled by approx. 5 pixels for low resolution gratings

Spectroscopy(sensitivity)



5- σ sensitivity in 30 minutes on-source in 10- μ m low-resolution spectroscopy mode.



5- σ sensitivity in 30 minutes on-source in 20- μ m low-resolution spectroscopy mode.

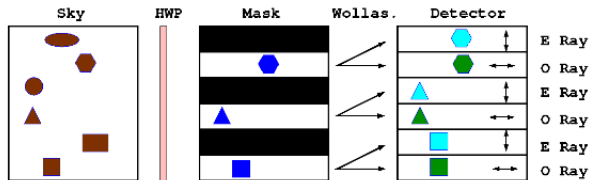
Spectroscopy(sensitivity)

At bluer wavelengths, where the PSF is narrower, there is a higher contribution from the background within the aperture than at redder wavelengths

In the case of $20\ \mu m$ window there is a stronger dependency of the sensitivity with wavelength than in the $10\ \mu m$ window, due to the presence of strong water lines in the $20\ \mu m$ atmospheric window.

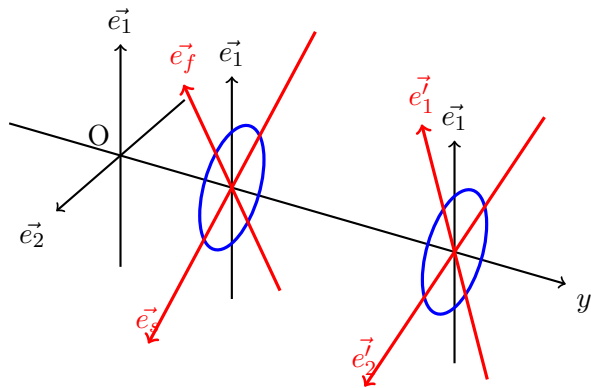
Polarimetry

- half wave plate (retarder with $\delta = \pi$)
- a focal plane mask which prevents overlap of the orthogonally polarized images for extended sources
- cadmium selenide (CdSe) Wollaston prism (an optical device which separates unpolarized light into two orthogonal linearly polarized outgoing beams)



Sketch of how dual-beam imaging polarimetry works. The light any object of the sky, which can or cannot be polarized, passes through the HWP. The HWP polarizes the beam linearly in one direction. Then the polarization mask selects only half of the FOV. Finally the beam is split in ordinary and extraordinary rays (O and E rays).

Polarimetry



- \vec{e}_1, \vec{e}_2 reference system in object plane
- α angle between \vec{e}_1 and \vec{e}_f the fast axis of the retarder
- β angle between \vec{e}_1 and \vec{e}'_1 one of the orthogonal axis of the wollaston prism: for example O-ray
- δ phase difference between fast and slow axis induced by the retarder (π in case of HWP)

- at the entrance of the retarder in basis \vec{e}_1, \vec{e}_2 :
 - $E_1 = \epsilon_1 e^{-i\omega t}$
 - $E_2 = \epsilon_2 e^{-i\omega t}$
- rotation (in slow axis, fast axis basis: S.R of the retarder)
 - $E_f = (\epsilon_1 \cos\alpha + \epsilon_2 \sin\alpha) e^{-i\omega t}$
 - $E_s = (-\epsilon_1 \sin\alpha + \epsilon_2 \cos\alpha) e^{-i\omega t}$
- at the exit of the retarder (in the same basis: S.R of the retarder)
 - $E_f = (\epsilon_1 \cos\alpha + \epsilon_2 \sin\alpha) e^{-i\omega t}$
 - $E_s = (-\epsilon_1 \sin\alpha + \epsilon_2 \cos\alpha) e^{i\delta} e^{-i\omega t}$
- at the exit of the retarder (rotation $\beta - \alpha$: in the S.R. of the wollaston prism) the component along \vec{e}_1' :
 $E_1' = \cos(\beta - \alpha) E_f + \sin(\beta - \alpha) E_s \implies$
 $E_2' = -\sin(\beta - \alpha) E_f + \cos(\beta - \alpha) E_s \implies$

$$E_1' = [\cos(\beta - \alpha)(\epsilon_1 \cos\alpha + \epsilon_2 \sin\alpha) + \sin(\beta - \alpha)(-\epsilon_1 \sin\alpha + \epsilon_2 \cos\alpha) e^{i\delta}] e^{-i\omega t} \quad (1)$$

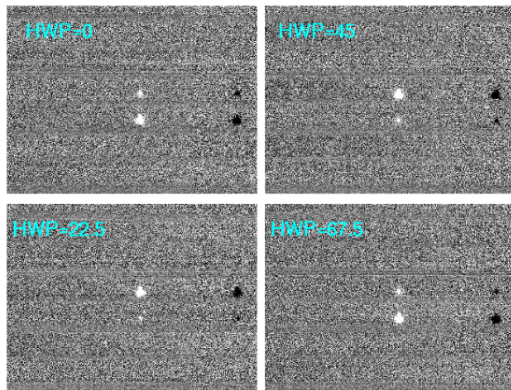
- $I \propto \epsilon_1 \epsilon_1^* + \epsilon_2 \epsilon_2^*$
- $Q \propto \epsilon_1 \epsilon_1^* - \epsilon_2 \epsilon_2^*$
- $U \propto \epsilon_1^* \epsilon_2 + \epsilon_1 \epsilon_2^*$
- $V \propto i(\epsilon_1^* \epsilon_2 - \epsilon_1 \epsilon_2^*)$
- signal O-ray (polarized along \vec{e}_1') $\propto \langle E_1' E_1'^* \rangle \propto$
 $\frac{1}{2}[I + (Q \cos 2\alpha + U \sin 2\alpha) \cos(2(\beta - \alpha))$
 $- (Q \sin 2\alpha - U \cos 2\alpha) \sin(2(\beta - \alpha)) \cos \delta$
 $+ V \sin(2(\beta - \alpha)) \sin \delta]$

$\delta = 180^\circ, \beta$ fixed \implies in order to recover Stokes parameters we need 4 different values of α : the HWP rotates automatically (synchronized with the chopping and nodding) between the four position angles of $0^\circ, 45^\circ, 22.5^\circ$ and 67.5°

Chop and nod

To alleviate the effects of the bright background in mid-IR when performing imaging and low-resolution spectroscopy, a nearby position on the sky is observed frequently by moving the secondary mirror at a frequency of a few Hz (the telescope is said to chop between the target position and an adjacent sky position), and the pairs of images are subtracted. Moving the secondary mirror results in the telescope being seen by the detector in slightly different ways in the two secondary mirror positions. Since the telescope glows strongly at mid-IR wavelengths the subtraction leaves a residual radiative offset, which is much less than the telescope and sky brightnesses but is still significant. To get rid of (most of) this offset the entire telescope is moved or nodded typically about twice per minute. Normally the nod is set to be the same amplitude and direction as the chop, so that the science target switches chop positions between the two nod positions.

Polarimetry



Raw polarization image extensions corresponding to the first nod position in an observation of an unpolarized standard star for which a 100% linear polarization has been imposed by introducing a wire-grid in the optical path. The HWP angle rotates from one extension to the next, which causes the brightness of the ordinary and extraordinary images of the star (upper and lower images of the star in each image, respectively) to change from one HWP angle to the next, since the source is polarized. The same observation of an unpolarized source would show the same intensity in both rays. A chop/nod throw of $10''$ along the polarization mask slots was used. Therefore, both, the negative and positive images of the star can be seen because the on-source and off-source chopping images were subtracted.

Chop methods

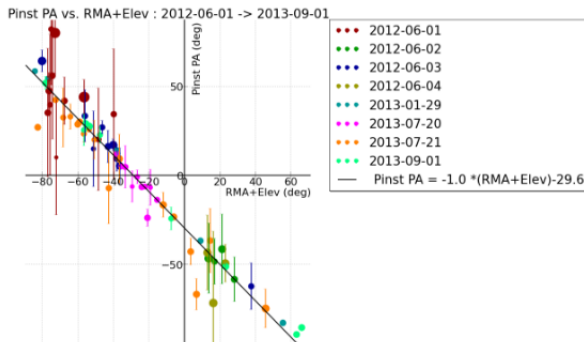
- The secondary mirror of the telescope is then moved slightly away from the nominal position so that the program object moves out of the field of view of the camera and another set of images is acquired. This procedure, called a chop cycle, is repeated many times at typically a 2-10 Hz rate moving back and forth between "on-source" and "off-source" positions. A "chop-differenced" signal is formed by taking the difference between the on-source and off-source images.
- In the on-chip method, the chopper throw is set to be less than the detector array field-of-view so that the source remains "on chip" in both chopper positions, i.e. in both the "on-source" and "off-source" chopper positions as referred to in the standard method. Note that since the source is present in both positions of the chopper, the chop-differenced frame will contain both a positive and negative image of the source

- dual beam polarimetry in N band window with accuracy $> 99\%$ at the center wavelength $10.5\mu m$
- decreasing towards the cutoff wavelength of N window
- 50% field of view blocked by the mask (to avoid overlapping of orthogonally polarized beams emerging from the prism)
- 2 beams \implies high precision (the difference from standard polarimeter with 1 exit beam - along acceptance axis)

- SNR needed in order to reach a certain polarization accuracy ΔP is given by:
- $SNR = \frac{\sqrt{2}}{\Delta P}$
- for example for a target with an expected polarization degree of 3% we want a polarization accuracy of 1% $\implies SNR = 141$
- we use the SNR afterwards when calculating exposure time in the Canaricam Exposure Time Calculator

| Filter | Polarization Efficiency (%) |
|----------|-----------------------------|
| Si1-7.8 | 72.1 |
| Si2-8.7 | 90.0 |
| Si3-9.8 | 97.3 |
| Si4-10.3 | 99.2 |
| Si5-11.6 | 95.5 |
| Si6-12.5 | 88.3 |

- degree of instrumental polarization $0.6 - 0.7\%$ across the N band window
- reflection(which induces linear polarization) at the GTC flat tertiary mirror (M3) with a 45 degree angle of incidence, which is expected to produce most of the instrumental polarization
- \implies polarization angle (PA) in table above varies with changing the instrument position angle (IPA) and when the elevation of star evolves with time



Dependency of the instrumental polarization angle with the RMA+Elev angle. The size of the symbols is proportional to the degree of polarization. The colors represent different dates. Observations with all Silicate filters and the N-10.36 filter are included in this plot. The values of RMA+Elev have been folded to be in the interval $[-90^\circ, 90^\circ]$.

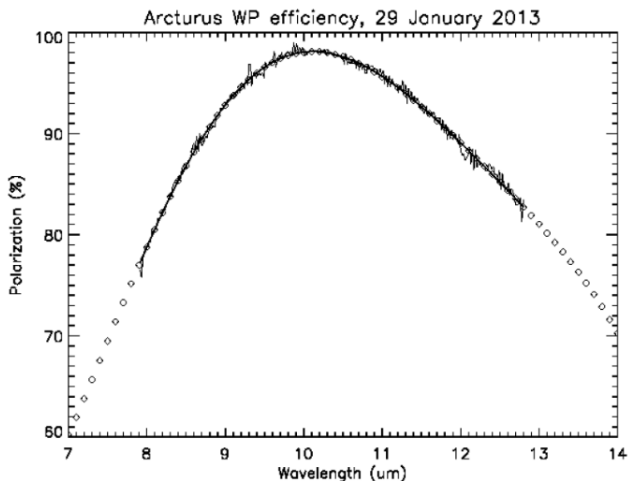
| 2013/07/20 - HD186791 - IPA=0° | | | | | | | |
|---------------------------------|----------|-------|----------------------|--------|-----------------------|------|----------------------|
| Filter | FWHM (") | P (%) | P _{Err} (%) | PA (°) | PA _{Err} (°) | SNR | P _{Acc} (%) |
| Si1-7.8 | 0.22 | 0.46 | 0.16 | -6.6 | 10.1 | 1061 | 0.13 |
| Si2-8.7 | 0.18 | 0.66 | 0.02 | -6.1 | 0.9 | 8001 | 0.02 |
| Si3-9.8 | 0.28 | 0.59 | 0.08 | -0.7 | 3.8 | 2123 | 0.07 |
| Si4-10.3 | 0.26 | 0.70 | 0.03 | -13.6 | 1.3 | 5350 | 0.02 |
| Si5-11.6 | 0.29 | 0.41 | 0.14 | -6.1 | 8.8 | 1332 | 0.11 |
| Si6-12.5 | 0.32 | 0.76 | 0.30 | 4.9 | 11.9 | 563 | 0.25 |
| N-10.36 | 0.37 | 0.71 | 0.03 | 5.3 | 1.2 | 5795 | 0.02 |
| 2013/07/21 - HD161096 - IPA=90° | | | | | | | |
| Filter | FWHM (") | P (%) | P _{Err} (%) | PA (°) | PA _{Err} (°) | SNR | P _{Acc} (%) |
| Si1-7.8 | 0.18 | 0.54 | 0.21 | 20.2 | 10.9 | 832 | 0.17 |
| Si2-8.7 | 0.24 | 0.59 | 0.03 | 26.0 | 1.3 | 6896 | 0.02 |
| Si3-9.8 | 0.26 | 0.69 | 0.12 | 23.6 | 4.9 | 1560 | 0.09 |
| Si4-10.3 | 0.26 | 0.87 | 0.05 | 28.9 | 1.5 | 3857 | 0.04 |
| Si5-11.6 | 0.29 | 0.64 | 0.17 | 33.2 | 7.1 | 1138 | 0.13 |
| Si6-12.5 | 0.32 | 0.68 | 0.39 | 32.7 | 16.6 | 470 | 0.30 |
| N-10.36 | 0.27 | 0.71 | 0.05 | 42.6 | 1.5 | 4653 | 0.03 |

Instrumental polarization measured in two different nights. The columns represent the (1) filter name, (2) FWHM of the PSF in the image, (3) percentage of polarization (P), (4) error in P, (5) polarization angle (PA), (6) error in the PA, (7) SNR of the data, (8) expected polarization accuracy from the measured SNR.

- the design permits having simultaneously the diffraction grating and the polarimeter
- the 2 beams (linearly polarized in orthogonal directions) emerging from the polarizer (Wollaston prism) : are imaged on the detector as separate spectra because the diffraction grating is also in the optical path (afterwards)
- as in polarimetry the field of view is reduced by 50%
- The same formula as in the case of imaging polarimetry relates the SNR needed to reach a given polarization accuracy , but in this case the calculation must be done for each spectral resolution element
- instrumental polarization consistent with imaging polarimetry results

Spectropolarimetry

Polarization Measurement Efficiency consistent with the efficiency table before (polarimetry)



Wave plate efficiency curve measured with CanariCam in spectropolarimetry mode together with a polynomial fit to the data (diamonds).

- detect faint mid-IR point sources, such as sub-stellar objects, and faint extended sources, such as circumstellar disks, that are located very close to bright point sources and which might not be detectable without the coronagraphic mode
- occulting spot mask at the telescope focal plane: sharp-edged (top hat), opaque metal disk with a radius of 0.84 arcsec ($\frac{r}{f}$)
- pupil mask at the first pupil plane inside camera: small central opaque disk for the central obscuration supported by thin, slightly wedged, veins that mask the images of the secondary mirror spider supports (and we need to keep them masked) + large hexagonally shaped mask that blocks the outer edges of the primary mirror

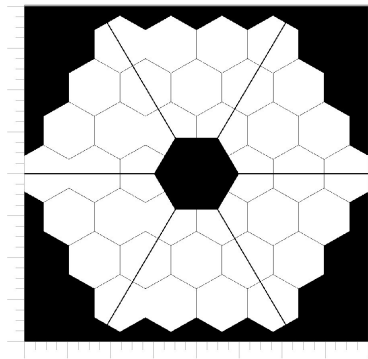


Figure 1: The shape of the GTC primary mirror